Molecular Cancer Therapeutics

Identification of the Serine Biosynthesis Pathway as a Critical Component of BRAF Inhibitor Resistance of Melanoma, Pancreatic, and Non–Small Cell Lung Cancer Cells

Kayleigh C. Ross[1], Andrew J. Andrews[1,2], Christopher D. Marion[1], Timothy J. Yen[2], and Vikram Bhattacharjee[1]

Abstract

Metastatic melanoma cells commonly acquire resistance to *BRAF* V600E inhibitors (BRAFi). In this study, we identified serine biosynthesis as a critical mechanism of resistance. Proteomic assays revealed differential protein expression of serine biosynthetic enzymes PHGDH, PSPH, and PSAT1 following vemurafenib (BRAFi) treatment in sensitive versus acquired resistant melanoma cells. Ablation of PHGDH via siRNA sensitized acquired resistant cells to vemurafenib. Inhibiting the folate cycle, directly downstream of serine synthesis, with methotrexate also displayed similar sensitization. Using the DNA-damaging drug gemcitabine, we show that gemcitabine pretreatment sensitized resistant melanoma cells to BRAFis vemurafenib and dabrafenib. We extended our findings to BRAF WT tumor cell lines that are intrinsically resistant to vemurafenib and dabrafenib. Pretreatment of pancreatic cancer and non–small cell lung cancer cell lines with sublethal doses of 50 and 5 nmol/L of gemcitabine, respectively, enhanced killing by both vemurafenib and dabrafenib. The novel aspects of this study are the direct identification of serine biosynthesis as a critical mechanism of *BRAF* V600E inhibitor resistance and the first successful example of using gemcitabine + BRAFis in combination to kill previously drug-resistant cancer cells, creating the translational potential of pretreatment with gemcitabine prior to BRAFi treatment of tumor cells to reverse resistance within the mutational profile and the WT. *Mol Cancer Ther; 16(8); 1596–609. ©2017 AACR.*

Introduction

Vemurafenib and dabrafenib are inhibitors of the MAPK pathway that are used to treat a variety of cancers that express the V600E *BRAF* mutant (1). The compounds received FDA approval in 2011 (vemurafenib) and 2013 (dabrafenib) for the treatment of unresectable or metastatic melanoma with oncogenic *BRAF* V600E mutations, which accounts for >60% of all melanoma cases (2). Vemurafenib and dabrafenib are contraindicated for BRAF wild-type melanoma because they exert paradoxical effects of promoting proliferation and migration through ERK1/2, thus making the drugs specific for *BRAF* V600E mutants (3, 4). Initially, BRAF inhibitors were shown to induce tumor regression. However, patients relapsed due to tumor-acquired resistance (5, 6). Several cellular pathways have been implicated in melanoma-acquired resistance to BRAF inhibitors including hyperactivation of EGFR pathway tyrosine kinases (7), hyperactivation of MEK1/2 (8, 9) and/or ERK1/2 (10), and induction of compensatory resistance pathways mTOR and PI3K (11, 12). Indeed, MEK1/2 inhibitors in combination with *BRAF* V600E inhibitors have initially demonstrated clinical effectiveness (13, 14), but patients also developed acquired resistance to this combination (14, 15). Despite therapies targeting the BRAF/MEK/ERK cascade, 5-year survival for metastatic melanoma remains <20%. Therefore, the need to understand and reverse mechanisms of acquired cancer cell resistance to kinase inhibitors and other classes of drugs remains a priority.

In this study, we identified proteins and pathways responsible for melanoma acquired resistance to vemurafenib. We established a vemurafenib-resistant melanoma cell line, SK-MEL-28VR1, from parental *BRAF* V600E SK-MEL-28 cells. We compared proteomic profiles of drug-resistant versus sensitive cells by mass spectrometry (MS) to identify mechanisms of drug resistance with an agnostic, label-free method and proprietary bioanalytic software. MS data revealed that serine biosynthesis pathway enzymes were differentially expressed between the two cell lines following vemurafenib treatment. Serine biosynthesis is known to be upregulated in cancer cells as a mechanism contributing to enhanced nucleotide synthesis (16). Protein abundances of all enzymes of the pathway [D-3-phosphoglycerate hydrogenase (PHGDH), phosphoserine aminotransferase 1 (PSAT1), and phosphoserine phosphatase (PSPH)] increased or stayed the same in response to vemurafenib in SK-MEL-28VR1 cells yet decreased in SK-MEL-28 cells. siRNA knockdown of PHGDH and serine depletion experiments established serine synthesis as a critical component for vemurafenib resistance in SK-MEL-28VR1 cells.

[1]Evol Science, Philadelphia, Pennsylvania. [2]Fox Chase Cancer Center, Philadelphia, Pennsylvania.

Note: Supplementary data for this article are available at Molecular Cancer Therapeutics Online (http://mct.aacrjournals.org/).

Corresponding Author: Vikram Bhattacharjee, Evol Science, LLC, 3624 Market Street, Suite 5E, Philadelphia, PA 19104. Phone: 215-966-6102; Fax: 215-966-6002; E-mail: vikram@evolscience.com

doi: 10.1158/1535-7163.MCT-16-0798

Data showed serine biosynthesis to be upregulated in SK-MEL-28VR1 cells, but not in parental cells, in response to vemurafenib. In addition, methotrexate experiments showed that the folate cycle, immediately downstream of serine biosynthesis, can be inhibited to sensitize SK-MEL-28VR1 cells to vemurafenib. As nucleotides synthesized from the folate cycle contribute to DNA damage response and repair, we tested the DNA-damaging agent gemcitabine in combination with vemurafenib and vemurafenib + methotrexate on SK-MEL-28VR1 cells. Indeed, SK-MEL-28VR1 cells were sensitized to vemurafenib following gemcitabine addition. This sensitization was enhanced by methotrexate. Importantly, the order of drug addition was critical for sensitization. Cells had to be pretreated with gemcitabine for 24 hours before exposure to vemurafenib or vemurafenib + methotrexate. Next, we tested the gemcitabine + vemurafenib combination in BRAF WT cancer cells. We found 1 pancreatic cancer and 1 non–small cell lung cancer (NSCLC) cell line that exhibited similar responses as SK-MEL-28VR1 cells. In summary, we have identified serine biosynthesis as a critical component of vemurafenib acquired and intrinsic resistance in cancer cells. We have demonstrated combinational therapy potential using gemcitabine to sensitize cancer cells to vemurafenib. In addition, methotrexate enhanced gemcitabine-induced sensitization of cancer cells to vemurafenib. Finally, we showed that gemcitabine can be used in combination with another *BRAF* V600E inhibitor dabrafenib to effectively kill cancer cells.

Materials and Methods

Cell culture and chemicals

Panc1, BxPC3, MiaPaca2, and NCI-H2122 cells were purchased from ATCC. ATCC authenticated cell lines by morphology checks, growth curve analysis, isoenzymology, and mycoplasma testing. SK-MEL-28 cells were a gift from Dr. Alfonso Bellacosa at Fox Chase Cancer Center (FCCC, Philadelphia, PA). SK-MEK-28 cells were authenticated by the FCCC cell culture core according to ATCC test recommendations. Cell line SK-MEL-28VR1 was identified through progressive vemurafenib selection. SK-MEL-28 cells (1×10^5) were exposed to 10 μmol/L vemurafenib for 48 hours, then 20 μmol/L of vemurafenib for 48 hours, then 30 μmol/L of vemurafenib for 48 hours. Surviving cells were pooled and identified as the SK-MEL-28VR1 cell line. Cell line BxPC3M1 was identified through passive selection of BxPC3 cells. Single BxPC3 cells were plated and allowed to grow in subclones. Subclones with detached phenotypes different from the highly adherent BxPC3 parental cells were identified and isolated as BxPC3M cell lines. One such cell line was BxPC3M1. All cell lines were reanimated less than 6 months before experimentation. Cell lines were cultured in DMEM/10%FBS (GenDepot) or RPMI1640/10%FBS (GenDepot) supplemented with 2 mmol/L glutamine (Life Technologies; 25030081) and were maintained at 37°C in 5% CO_2. RPMI1640 without glucose, glycine, or serine (Teknova)/10% Dialyzed FBS (Life Technologies; 26400036) were used for serine deprivation studies. Vemurafenib, dabrafenib, methotrexate, and gemcitabine were obtained from Selleckchem. PHGDH siRNA was obtained from Ambion (AM16708), and Lipofectamine RNAiMax from Invitrogen (100014472).

Cell viability assays

For colony formation assays, 400 cells/well were seeded into 24-well plates. Cells were treated with DMSO or gemcitabine at various doses on day 1 for 24 hours. Gemcitabine was washed out on day 2, vemurafenib, dabrafenib, and methotrexate were added. On day 4, drugs added on day 2 were washed out. Cells were allowed to grow for 7 days and fixed (10% methanol + 10% acetic acid) and stained with crystal violet (0.4% in 20% ethanol) for quantitation at 595 nm. For spheroid assays, cells were plated in 96-well spheroid plates (Corning CLS4515) according to cell line–specific plating efficiencies that allowed for >500 μm in diameter of spheroid after 48 hours. Cells were treated with DMSO or gemcitabine at various doses on day 2 for 24 hours. Cells exposed to gemcitabine were serially washed with warm media in order to remove any traces of gemcitabine from the cells prior to BRAFi addition. On day 5, growth was analyzed using CellTiter Glo 3D (Promega).

Mass spectrometry

Cells were harvested, washed in PBS, and lysed in NP40 lysis buffer (1% NP40/PBS/10% glycerol) with protease inhibitors. Detergents were removed from protein samples using columns (Pierce; 87777). Protein concentrations were determined with Total-Protein-Assay-kit (ITSI Biosciences; K-0014-20). Samples were prepared for MS using the OneKit (Evol Science). Briefly, 100 μg of protein sample + 5 μg normalization peptides were propionylated prior to overnight trypsin digestion. Another 100 μg of the protein sample with normalization peptides were trypsin digested overnight without propionylation. Samples were dried down and redissolved in 2.5% ACN/0.1% formic acid for liquid chromatography–tandem mass spectrometry (LC-MS/MS) analysis carried out on Q-Exactive HF (Thermo Fisher) coupled with U3000 RSLCnano HPLC device (Thermo Fisher). Five microliters of sample were loaded onto C_{18} trap columns (PepMap100; 300-μm intardermally × 5 mm, 5-μm particle size, 100 Å; Thermo Fisher) at flow rates of 10 μL/minute. Peptide separation was carried out on a C_{18} column (ACQUITY UPLC M-Class Peptide CSH C18; 130Å 1.7 μm 75 μm x 250 mm, Waters) at flow rates of 0.26 μL/minute and the following gradient: 0–3 minutes, 2% B isocratic; 3–76 minutes, 2%–30% B; 76–90 minutes, 30%–45% B; 90–98 minutes, 45%–98% B. Mobile phase A was 0.1% formic acid, and mobile phase B was 0.1% formic acid in 80:20 acetonitrile:water. The runs were analyzed using Progenesis-QI (Nonlinear dynamics). The chromatograms were aligned and the MS/MS data was extracted for peptide identification using Mascot (Matrix Science; v2.5.1). Mascot was set up to search the cRAP database, the custom database including the normalization peptide sequence, and SwissProt human database assuming trypsin digestion. Mascot was searched with fragment ion mass tolerance of 0.06 kDa and parent ion tolerance of 15 PPM. Deamidated asparagine and glutamine, oxidated methionine, acetylated lysine, propionylated lysine, and carbamidomethylated cysteine were specified in Mascot as variable modifications. The peptides identified using FDR < 1% were extracted and imported back into Progenesis for assignment of the peaks. Only proteins with ≥2 unique peptides and a Mascot score of 20 were used. The peptide and protein quantification used a synthetic control peptide for normalization across the samples. All MS runs were performed at the Donald Danforth Plant Science Center for Proteomics and Mass Spectrometry and at the Proteomics and Metabolomics facility at University of Nebraska (Lincoln, NE).

Data plotting and statistics

Proteomic trend plots were constructed using Evol Science Software suite (ESSv1.0). Volcano plotting visually separates data

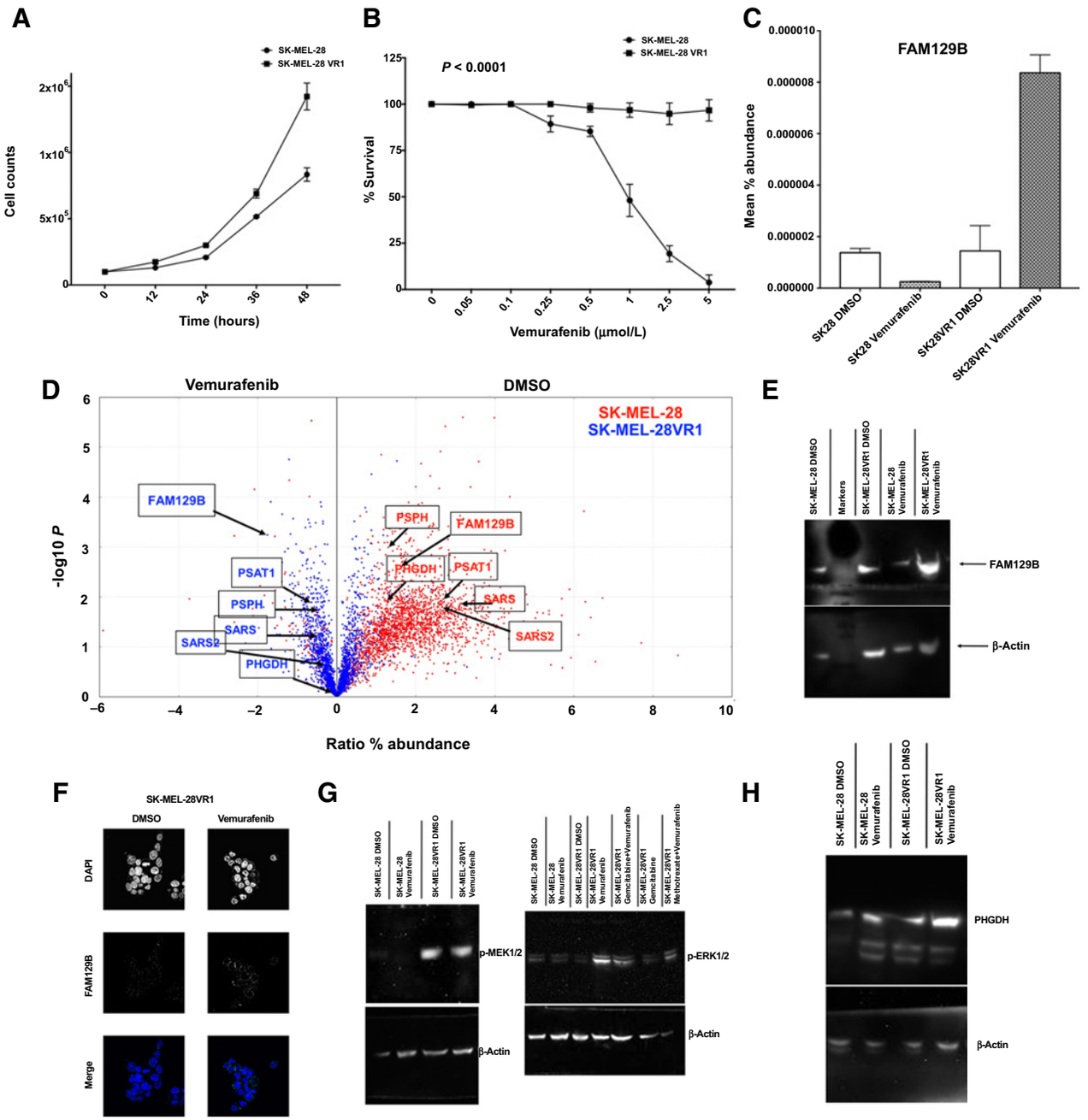

Figure 1.

Characterization of SK-MEL-28VR1 cells. **A,** Growth rate comparisons of SK-MEL-28 and SK-MEL-28VR1 cells ($n = 3$). A total of 1×10^5 cells were plated at time-point 0. **B,** Colony formation assays of SK-MEL-28 and SK-MEL-28VR1 cells following treatments with differential doses of vemurafenib ($n = 5$; $P < 0.0001$). **C,** Mass spectrometry: FAM129B protein abundance following differential treatments of SK-MEL-28 and SK-MEL-28VR1 cells ($n = 3$). **D,** Mass spectrometry: Volcano plot displaying differential protein expression following vemurafenib treatments. SK-MEL-28 protein expression is displayed in red; SK-MEL-28VR1 protein expression is displayed in blue ($n = 3$). Proteins displayed on the right side of 0 in the *x*-axis are decreasing in abundance with vemurafenib treatments, and proteins displayed on the left side of the 0 in the *x*-axis are increasing in abundance following vemurafenib treatments. **E,** Western blots of FAM129B protein expression in differentially treated SK-MEL-28 and SK-MEL-28VR1 cells. β-Actin used as loading control. Fifty micrograms of protein loaded in each lane. **F,** IF staining: SK-MEL-28VR1 cells were costained with DAPI and FAM129B primary antibody. Cells were treated with either vemurafenib (10 μmol/L) or DMSO for 48 hours prior to staining. **G,** Western blots of p-MEK1/2 and p-ERK1/2 protein expressions in differentially treated SK-MEL-28 and SK-MEL-28VR1 cells. β-Actin was used as a loading control. Fifty micrograms of protein loaded in each lane. **H,** Western blot analysis of PHGDH protein expression in differentially treated SK-MEL-28 and SK-MEL-28VR1 cells. β-Actin was used as loading control. Fifty micrograms of protein loaded in each lane.

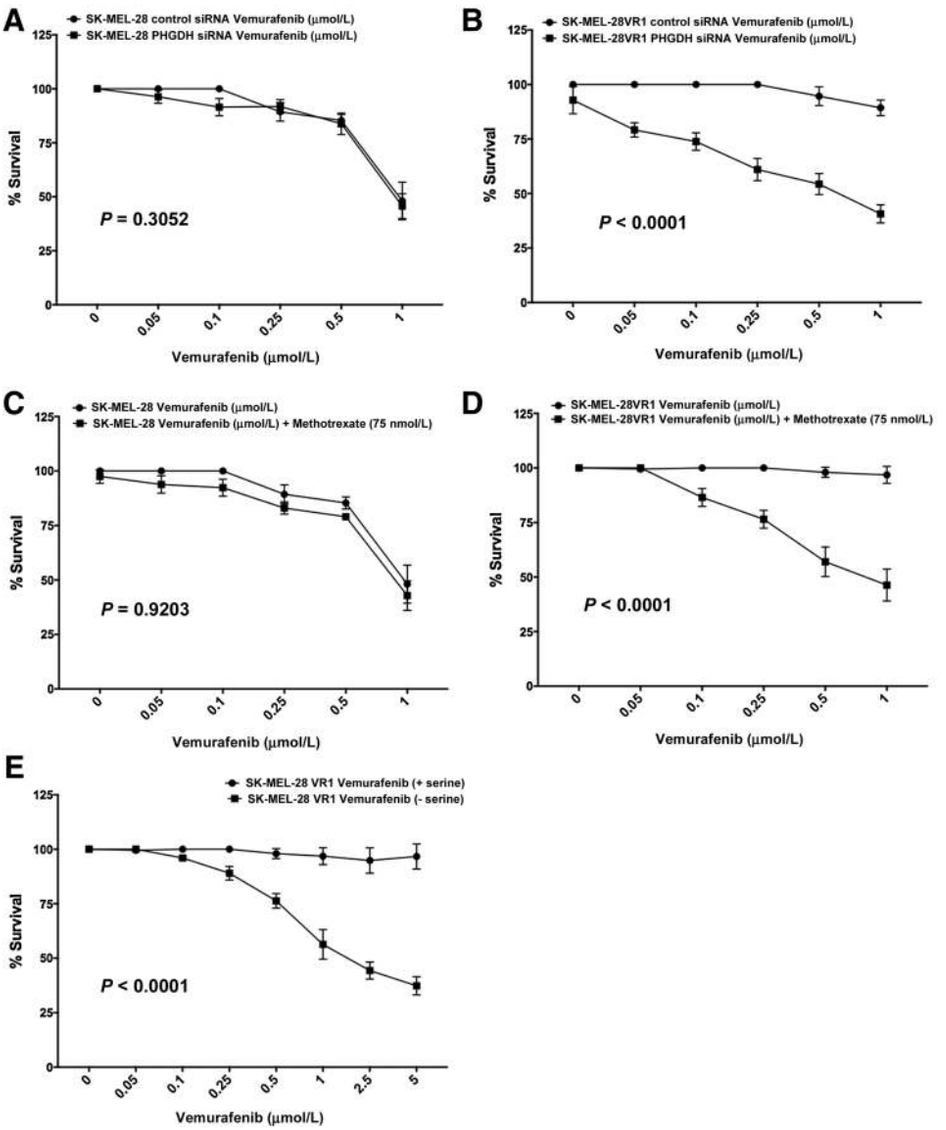

Figure 2.

Importance of serine biosynthesis pathway to vemurafenib resistance in SK-MEL-28VR1 cells. **A,** Colony formation assays of SK-MEL-28 cells following control or PHGDH siRNAs treatments with differential doses of vemurafenib ($n = 3$; $P = 0.3052$). **B,** Colony formation assays of SK-MEL-28VR1 cells following control or PHGDH siRNAs treatments with differential doses of vemurafenib ($n = 3$; $P < 0.0001$). **C,** Colony formation assays of SK-MEL-28 cells following treatments with differential doses of vemurafenib ± methotrexate (75 nmol/L; $n = 3$; $P = 0.9203$). **D,** Colony formation assays of SK-MEL-28VR1 cells following treatments with differential doses of vemurafenib ± methotrexate (75 nmol/L; $n = 3$; $P < 0.0001$). **E,** Colony formation assays of SK-MEL-28VR1 cells following treatments with differential doses of vemurafenib ± serine in media ($n = 3$; $P < 0.0001$).

points in axes by expression ratio and statistical significance. This enables a method of determining the significant, differentially expressed proteins within a comparison. For each protein, replicate values are compared creating two distributions of values. Student *t* test of identical mean is used between the two independent samples of values to compare distributions and generate *P* values of statistical significance. The –log10 of the *P* value is then taken to provide the Y coordinate, in graphical view. The X coordinate, ratio, is given by the log10 of the average of replicate ratio values for a given experiment. Combination index calculations, Fa-CI plots, and isobolograms were constructed using the CompuSyn software using the Chou–Talalay method (17). All cell culture assay plots were constructed using Prism7 software (Graphpad.com), and two-way ANOVA tests were used to calculate *P* values.

Immunoblotting

Cells were harvested and lysed in buffer (1% NP40/PBS/10% glycerol) with protease and phosphatase inhibitors. Protein concentrations were determined with Total-Protein-Assay-kit (ITSI Biosciences; K-0014-20) and then SDS sample buffer was added to the lysates. Fifty micrograms of boiled lysates were separated by

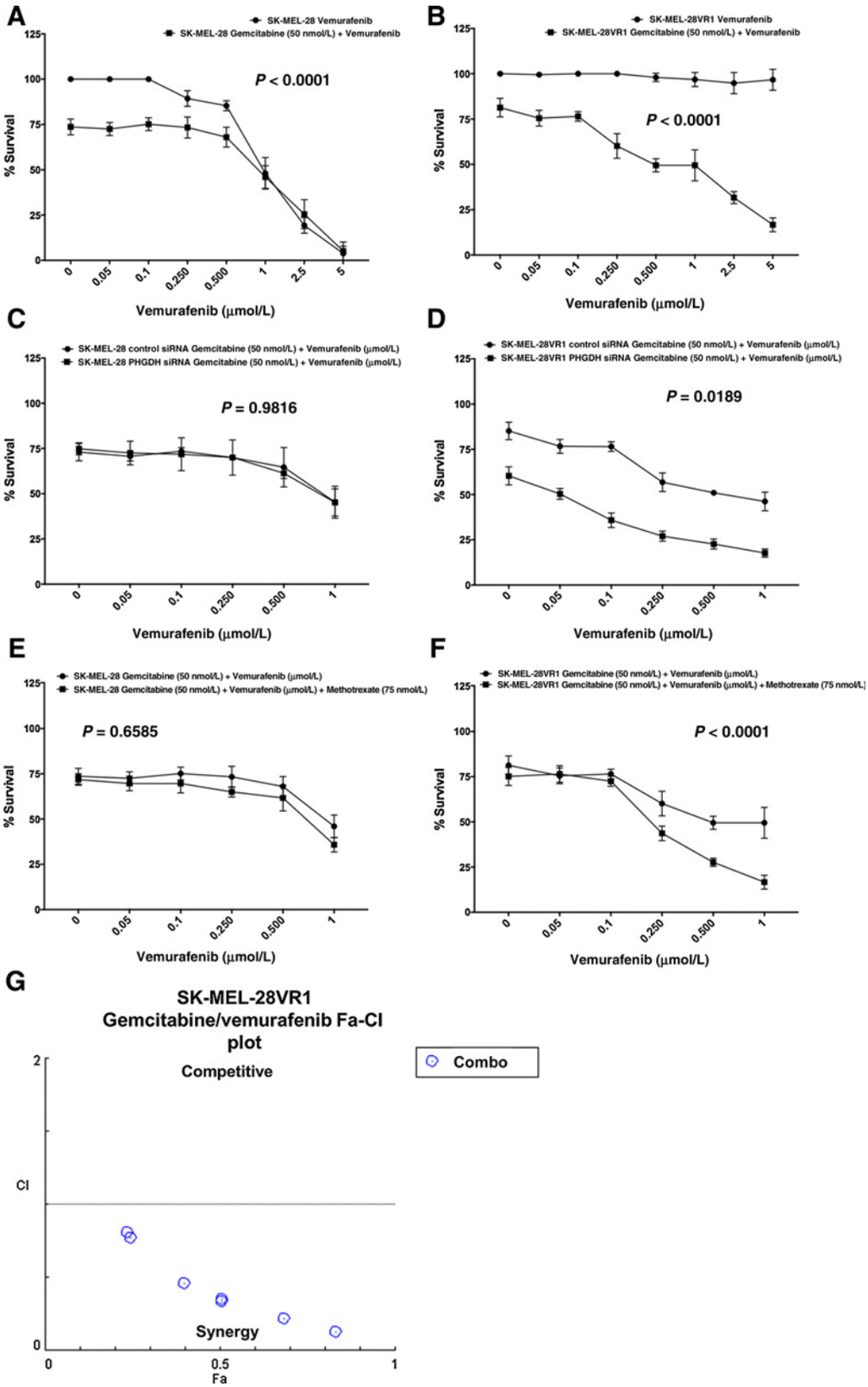

SDS-PAGE and transferred onto Immobilon P membranes (Millipore; IPVH00010). PHGDH primary antibody was obtained from Bethyl Laboratories (A304-732A). p-ERK1/2 (4370), p-MEK1/2 (9154), FAM129B (5122) primary antibodies were obtained from Cell Signaling Technology. β-Actin (Cell Signaling Technology 8457) and α-tubulin (Abcam ab7291) primary antibodies were used as loading controls. Anti-rabbit IgG, HRP-linked antibody (Cell Signaling Technology 7074) was used as the secondary antibody.

Immunofluorescence microscopy

Cells were plated onto coverslips. On day 1, cells were treated with DMSO or drug. On day 3, cells were fixed (4% paraformaldehyde), permeabilized, blocked, stained according to Cell Signaling Technology immunofluorescence (IF) protocols. Cells were permeabilized with 0.2% Triton X-100 for 15 minutes at room temperature. Cells were blocked with 3% BSA for 1 hour at room temperature. Primary antibody incubation with rabbit FAM129B (Cell Signaling Technology 5122) overnight at 4°C. Alexa Fluor–conjugated anti-rabbit (488 nm) secondary antibody (Jackson Laboratories 111-545-003) was used at a concentration of 1.5 μg/mL and nuclei counterstained with DAPI. Images were taken using a Leica Microsystems TCS-SP8A confocal microscope controlled by LAS software (Biological imaging facility, FCCC, Philadelphia, PA).

Results

Identification and characterization of vemurafenib-resistant SK-MEL-28VR1 cells

SK-MEL-28 vemurafenib-resistant cell line was isolated from SK-MEL-28 parental cells via drug selection. Proliferation rate of SK-MEL-28VR1 was higher than parental cells (Fig. 1A). SK-MEL-28VR1 cells had doubling times of 16 hours while parental cells had doubling times of 23.1 hours. Colony formation assays revealed that SK-MEL-28VR1 cells are vemurafenib-resistant (Fig. 1B). Mass spectrometry (MS) analysis revealed that SK-MEL-28VR1 had a different proteomic profile than parental cells in response to vemurafenib treatment. FAM129B was identified as having the third highest differential expression between SK-MEL-28VR1 cells treated with vemurafenib versus SK-MEL-28VR1 cells treated with vehicle (Supplementary Table S1). Cytoplasmic FAM129B abundance increased by approximately 6-fold with vemurafenib compared with vehicle (Fig. 1C). Interestingly, FAM129B abundance decreased in response to vemurafenib in parental cells (Fig. 1C and D). These trends indicated an active MAPK pathway (18) in SK-MEL-28VR1 cells but not in parental cells. Immunoblotting and IF staining of cytosolic protein extracts probing for FAM129B confirmed observed MS trends of increased protein expression following vemurafenib treatments of SK-MEL-28VR1 cells (Fig. 1E and F). Blots using MAPK protein p-MEK1/2 and p-ERK1/2 primary antibodies confirmed MAPK activation indicated by the increase in activating phosphorylation of ERK1/2 following vemurafenib treatment in SK-MEL-28VR1 cells but not in parental cells (Fig. 1G). Interestingly, MEK1/2 phosphorylation increased following vemurafenib treatments in both cell lines (Fig. 1G). Furthermore, FAM129B protein trends supported the observed induction of cell proliferation and suggested an invasive potential increase of SK-MEL-28VR1 cells.

Serine biosynthesis pathway proteins were the highest differentially expressed proteins within a pathway between resistant and sensitive cells in response to vemurafenib. All enzymes of the pathway (PHGDH, PSAT1, and PSPH) and serine-tRNA ligases SARS (cytoplasmic) and SARS2 (mitochondrial) were expressed in equal or higher abundances in SK-MEL-28VR1 cells exposed to vemurafenib than to vehicle, while the opposite trend was observed in parental cells (Fig. 1D). Immunoblotting using PHGDH antibody confirmed trends observed with MS (Fig. 1H). Consistent with MS data, Western blot analyses revealed SK-MEL-28VR1 cells having increased baseline PHGDH expression compared with parental cells. In addition, Western blot analyses revealed that PHGDH levels increased following vemurafenib treatment in SK-MEL-28VR1 cells (Fig. 1D and H).

PHGDH is essential for vemurafenib resistance of SK-MEL-28VR1 cells

PHGDH catalyzes the conversion of 3-phosphoglycerate to 3-phosphohydroxypyruvate comprising step 1 of the serine synthesis pathway. To directly test whether serine synthesis was critical for vemurafenib resistance, we used siRNAs to deplete PHGDH in SK-MEL-28VR1 and SK-MEL-28 cells (Supplementary Fig. S1). PHGDH siRNAs enhanced SK-MEL-28VR1 cell death following vemurafenib treatment while not having any additive effect on parental cell death (Fig. 2A and B). Control siRNA treatments established baseline cell viability following vemurafenib treatment for each cell line. PHGDH siRNA + vemurafenib treatments exhibited decreased cell viability below the baseline in SK-MEL-28VR1 cells (Fig. 2B) but not in parental cells (Fig. 2A).

Methotrexate selectively sensitizes SK-MEL-28VR1 cells to vemurafenib

As serine biosynthesis proteins are induced in SK-MEL-28VR1, we investigated whether serine synthesis was contributing precursors downstream to the folate cycle. The folate cycle is necessary for the production of tetrahydrofolate (THF) leading to the production of thymidylate which is critical for DNA synthesis and repair in cancer cells (19). In addition, the same study demonstrated that conversion of serine to glycine and the folate cycle contribute precursors to one-carbon ATP production in the

Figure 3.

Gemcitabine sensitizes SK-MEL-28VR1 cells to vemurafenib. **A,** Colony formation assays of SK-MEL-28 cells following treatments with differential doses of vemurafenib ± gemcitabine (50 nmol/L; $n = 3$) ($P < 0.0001$). **B,** Colony formation assays of SK-MEL-28VR1 cells following treatments with differential doses of vemurafenib ± gemcitabine (50 nmol/L; $n = 3$; $P < 0.0001$). **C,** Colony formation assays of SK-MEL-28 cells following control or PHGDH siRNAs treatments with differential doses of vemurafenib ± gemcitabine (50 nmol/L; $n = 3$; $P = 0.9816$). **D,** Colony formation assays of SK-MEL-28VR1 cells following control or PHGDH siRNAs treatments with differential doses of vemurafenib ± gemcitabine (50 nmol/L; $n = 3$; $P = 0.0189$). **E,** Colony formation assays of SK-MEL-28 cells following treatments with differential doses of vemurafenib + gemcitabine (50 nmol/L) ± methotrexate (75 nmol/L; $n = 3$; $P = 0.6585$). **F,** Colony formation assays of SK-MEL-28VR1 cells following treatments with differential doses of vemurafenib + gemcitabine (50 nmol/L) ± methotrexate (75 nmol/L; $n = 3$; $P < 0.0001$). **G,** Fa-CI plot representing synergy between gemcitabine and vemurafenib. Data points falling below the line indicate synergy between drugs. Data points represent CI calculations at specific doses. Please refer to Supplementary Table S2 for CI values.

cytosol of tumor cell lines. Methotrexate inhibits dihydrofolate reductase and thymidylate synthase thus reducing nucleotide synthesis (20). Methotrexate has also been shown to reduce ATP levels in tumor cells (19). Consistent with the importance of serine to the folate cycle, methotrexate (75 nmol/L) enhanced killing of SK-MEL-28VR1 cells following vemurafenib treatment (Fig. 2D). No significant killing by methotrexate + vemurafenib treatments was observed in parental cells (Fig. 2C). We next tested whether sensitization via methotrexate was achieved by attenuating the ERK1/2–dependent proliferative pathway. In Fig. 1G, immunoblots showed an increase of p-ERK1/2 in SK-MEL-28VR1 cells treated with methotrexate + vemurafenib compared with DMSO-treated cells revealing an active MAPK pathway. Therefore, we postulate that disrupting folate cycle–based nucleotide synthesis in MAPK pathway–induced proliferative backgrounds causes cell death.

Serine depletion sensitizes SK-MEL-28VR1 cells to vemurafenib

As interrupting the folate cycle with methotrexate sensitized SK-MEL-28VR1 cells to vemurafenib, we examined the effect of extracellular serine depletion on resistance. We used serine, glucose, glycine-depleted media during cell plating and drug treatments of SK-MEL-28VR1 cells in colony formation assays. Cells were then resupplied with complete media and colony growth commenced. The data showed depletion of serine for 2 days as sufficient to enhance killing of SK-MEL-28VR1 by vemurafenib (Fig. 2E). At vemurafenib doses of 2.5 μmol/L and 5 μmol/L, SK-MEL-28VR1 cells showed >50% reduction in colony formation with serine depletion. These data show that baseline extracellular serine levels (in serum) are critical for vemurafenib survival of SK-MEL-28VR1 cells.

Identification of gemcitabine as a sensitizer of SK-MEL-28VR1 cells to vemurafenib

Folate cycle is critical for nucleotide production during DNA repair, and PHGDH, PSAT1, and PSPH protein levels have been shown to increase under conditions of genomic instability (21). Therefore, we tested several classes of DNA-damaging agents as potential sensitizers of SK-MEL-28VR1 cells to vemurafenib including DNA cross-linking agents, topoisomerase inhibitors, and nucleoside analogues. The nucleoside analogue gemcitabine sensitized SK-MEL-28VR1 cells to vemurafenib when used in combination but did not sensitize SK-MEL-28 cells (Fig. 3A and B). A static dose of 50 nmol/L gemcitabine was added to variable doses of vemurafenib in colony formation assays. Presence of pERK1/2 revealed an active MAPK pathway in cells treated with gemcitabine + vemurafenib combination when compared with gemcitabine alone (Fig. 1G). Depletion of PHGDH via siRNA treatments enhanced SK-MEL-28VR1 cell death beyond that observed with gemcitabine + vemurafenib combination treatments (Fig. 3D). In addition, methotrexate enhanced cell death of SK-MEL-28VR1 cells when treated alongside gemcitabine + vemurafenib (Fig. 3E and F). Synergy between gemcitabine and vemurafenib in SK-MEL-28VR1 cells was indicated by combination index (CI) analysis (Fig. 3G; Supplementary Fig. S2A; Supplementary Table S2; ref. 17).

Vemurafenib sensitizes pancreatic cancer and NSCLC cells to gemcitabine

As we reversed vemurafenib-acquired resistance of SK-MEL-28VR1 cells via pretreatment with gemcitabine, we tested the combination in BRAF WT cells intrinsically resistant to vemurafenib. Gemcitabine is the first-line therapy in pancreatic cancer. We tested 4 pancreatic cancer cell lines (BxPC3, Panc1, MiaPaca2, and BxPC3M1) for gemcitabine sensitization via vemurafenib treatment. Using variable gemcitabine doses and constant vemurafenib dose of 1 μmol/L, colony formation assays revealed that BxPC3M1 cells were sensitized to gemcitabine by vemurafenib (Fig. 4A). Synergy between gemcitabine and vemurafenib BxPC3M1 cells was indicated by CI analysis at specific doses (Fig. 4B; Supplementary Fig. S2B; Supplementary Table S3). The highest (5,000 nmol/L) and lowest (5 nmol/L and 10 nmol/L) gemcitabine doses displayed competitiveness between gemcitabine and vemurafenib. However, gemcitabine doses of 25 nmol/L–1,000 nmol/L displayed synergy between the two drugs. In addition, gemcitabine has also been effective in the treatment of advanced NSCLC especially in unfit patients (22). We tested stage 4 adenocarcinoma NSCLC cell line NCI-H2122. We observed that 1 μmol/L vemurafenib sensitized NCI-H2122 cells to gemcitabine (Fig. 4C).

Vemurafenib induces serine biosynthetic enzymes in pancreatic cancer cells

Next, we tested the effect of vemurafenib treatment on pancreatic cancer cell proliferation. All cell lines tested (BxPC3M1, BxPC3, Panc1, MiaPaca2) express BRAF WT. Vemurafenib treatment (10 μmol/L) resulted in increased proliferation of the cell lines (Fig. 5A–D), consistent with previous findings (3). As serine synthesis has been shown to correlate with increasing proliferation of tumor cells, we compared the proteomic profiles of the pancreatic cancer cell lines via MS. PHGDH, PSAT1, PSPH, and SARS protein abundance increased in all cell lines tested (Fig. 5E–H). The BxPC3M1 cells expressed the highest increase in protein abundance of all 4 proteins compared with the other cell lines tested. In addition, methotrexate treatments in combination with gemcitabine + vemurafenib increased cell death of BxPC3M1 and NCI-H2122 cells compared with gemcitabine + vemurafenib treatments without methotrexate (Fig. 5I and J). Next, we examined the effect of extracellular serine depletion on BxPC3M1 vemurafenib resistance. We used serine, glucose, and glycine-depleted media during cell plating and drug treatments of BxPC3M1 cells in colony formation assays. Cells were then supplied with complete media and colony growth commenced. Quantitation of colony formation assays revealed significant increases in BxPC3M1 cell death following vemurafenib treatments under serine-depleted conditions (Fig. 5K). At the 5 μmol/L vemurafenib dose, BxPC3M1 cells showed >50% cell death with serine-depleted media.

Dabrafenib, BRAF V600E inhibitor, sensitizes cancer cells to gemcitabine

Similar to vemurafenib, dabrafenib is a *BRAF* V600E inhibitor with efficacy against metastatic melanoma (23, 24). We tested dabrafenib effectiveness in sensitizing SK-MEL-28VR1, BxPC3M1, and NCI-H2122 cells. The first-line drug of each disease state was given in variable doses. Dabrafenib is considered a first-line therapy in metastatic melanoma with *BRAF* V600E mutations, while gemcitabine is a first-line therapy in pancreatic cancer and NSCLC. For SK-MEL-28VR1 cells, gemcitabine dose was kept constant at 50 nmol/L with variable doses of dabrafenib. In contrast, dabrafenib dose was kept constant at 1 μmol/L with variable doses of gemcitabine in pancreatic cancer and NSCLC cell

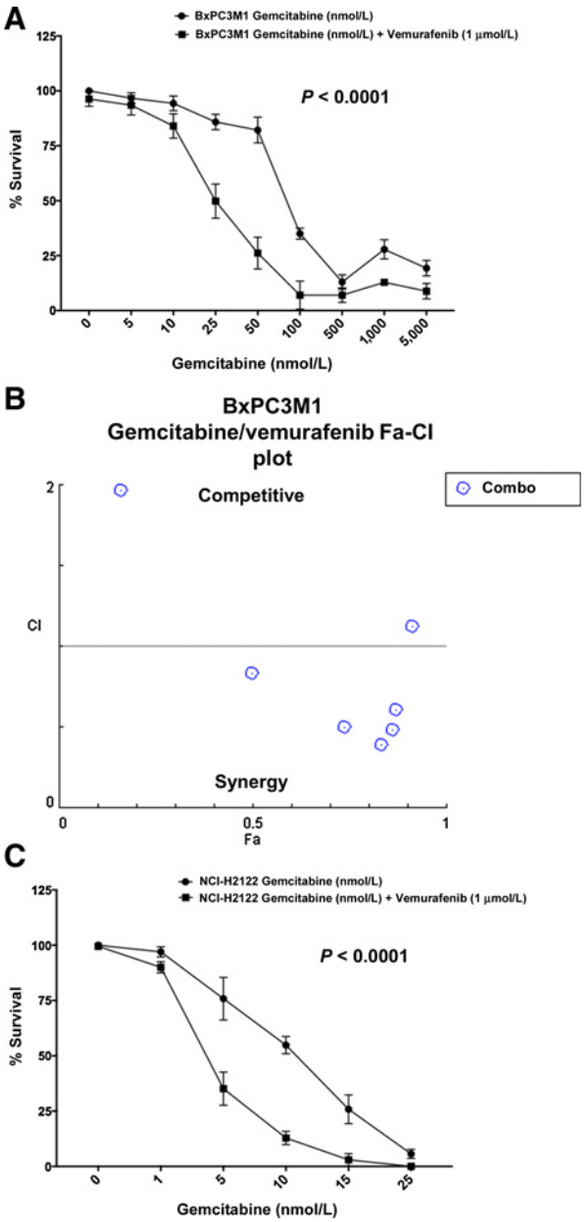

Figure 4.

Gemcitabine sensitizes pancreatic cancer and NSCLC cell lines to vemurafenib. **A,** Colony formation assays of BxPC3M1 cells following treatments with differential doses of gemcitabine ± vemurafenib (1 μmol/L; $n = 3$; $P < 0.0001$). **B,** Fa-CI plot representing synergy between gemcitabine and vemurafenib. Data points falling below the line indicate synergy between drugs. Data points represent CI calculations at specific doses. Please refer to Supplementary Table S3 for CI values. **C,** Colony formation assays of NCI-H2122 cells following treatments with differential doses of gemcitabine ± vemurafenib (1 μmol/L; $n = 3$; $P < 0.0001$).

lines. Dabrafenib treatment sensitized BxPC3M1 and NCI-H2122 cells to gemcitabine (Fig. 6A and B), and gemcitabine sensitized SK-MEL-28VR1 cells to dabrafenib (Fig. 6C). Finally, we tested the SK-MEL-28VR1 and BxPC3M1 cells in three-dimensional spheroid growth assays (Fig. 6D). This assay recapitulates some aspects of solid tumor growth *in vivo*. The spheroid assays clearly showed increased sensitivities of both cell lines to gemcitabine + dabrafenib combination treatments compared with dabrafenib treatment alone confirming colony formation data.

Discussion

We isolated vemurafenib-resistant SK-MEL-28 cells (SK-MEL-28VR1) to study mechanisms of *BRAF* V600E inhibitor resistance. MS data differentiated the protein signatures of SK-MEL-28VR1 cells from parental SK-MEL-28 cells in response to vemurafenib. Serine biosynthesis pathway enzyme levels were elevated in response to vemurafenib treatments of SK-MEL-28VR1 cells. In contrast, all proteins mentioned decreased in response to vemurafenib treatments of parental cells. Immunoblotting confirmed the trends observed from MS. We postulate that serine synthesis was critical for vemurafenib resistance of SK-MEL-28VR1 cells. Serine synthesis has been shown to be critical for cancer cell proliferation (25). Recent work by Labuschagne and colleagues showed that serine, not glycine, was critical for nucleotide and amino acid synthesis during cancer cell proliferation (25). SK-MEL-28VR1 cells had a higher proliferation rate (16-hour doubling time) compared with SK-MEL-28 cells (23.1-hour doubling time). Our proteomic observations of serine biosynthesis induction in response to vemurafenib in SK-MEL-28VR1 cells support published reports that positively correlate serine synthesis to cancer cell survival (26, 27).

Colony formation assays following PHGDH depletion via siRNA confirmed the importance of PHGDH gene products to SK-MEL-28VR1 resistance to vemurafenib. These data, along with colony formation assays following methotrexate treatments, confirmed that serine synthesis is a critical component of vemurafenib resistance signatures of SK-MEL-28VR1 cells. PHGDH catalyzes the first step of the serine biosynthesis pathway, converting 3-phosphoglycerate to 3-phosphohydroxypyruvate. Moreover, *PHGDH* gene amplifications have been reported in breast cancer and melanoma (28, 29). In fact, certain breast cancer cell types have shown to be dependent upon increased serine synthesis flux through higher PHGDH gene expression (27). In addition, in NSCLC, *PHGDH* gene overexpression positively correlates with aggressive disease (30). PHGDH gene expression is often amplified in metastatic melanoma and depletion of PHGDH negatively affects cell viability (31). The PHGDH depletion–induced vemurafenib sensitization is reminiscent of BRCA1 and platinum-based chemotherapy in breast cancer.

Serine biosynthesis lies upstream and feeds into multiple pathways involved in nucleotide and amino acid metabolism. Specifically, the folate cycle contributes to nucleotide metabolism. We tested the antifolate methotrexate in combination with vemurafenib on SK-MEL-28 and SK-MEL-28VR1 cell viability. Methotrexate selectively sensitized SK-MEL-28VR1 cells to vemurafenib. Methotrexate is known to inhibit the folate cycle downstream of serine biosynthesis in the alternative metabolic pathway known as SOG (Serine-One carbon cycle-Glycine cleavage), which is activated in cancer cells during proliferation (19). Serine depletion experiments demonstrated the need for baseline levels of extracellular serine for SK-MEL-28VR1 vemurafenib resistance. Recent work has identified the need for BRAF inhibitor–resistant melanoma cells to switch to oxidative metabolism during induction of cell proliferation (32). In fact, resistant cells are reported to be dependent on

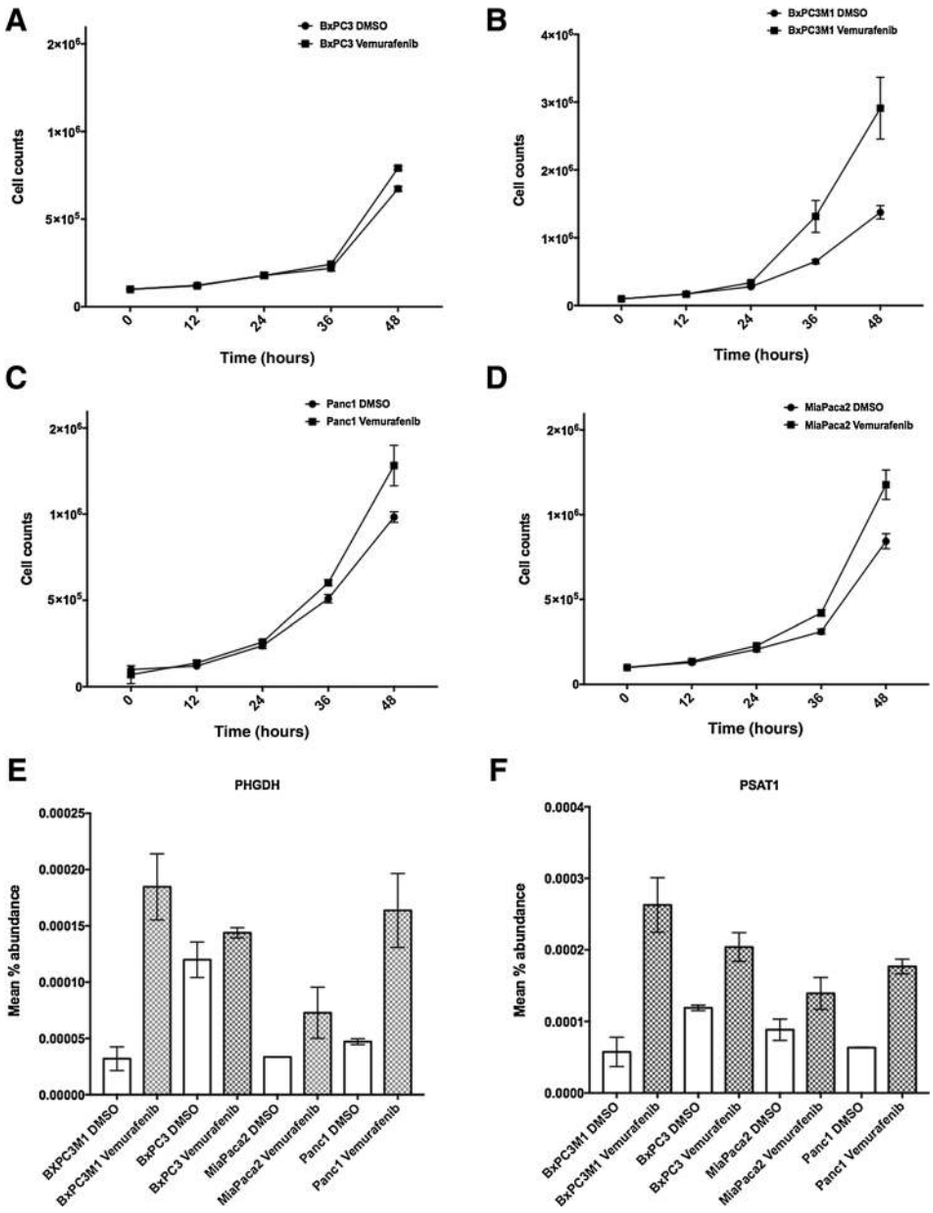

Figure 5.

Vemurafenib induces cell proliferation and serine synthesis in pancreatic cancer cell lines. **A,** Cell proliferation assay of BxPC3 cells treated with vemurafenib (10 μmol/L). A total of 1×10^5 cells were plated on day 0. **B,** Cell proliferation assay of BxPC3M1 cells treated with vemurafenib (10 μmol/L). A total of 1×10^5 cells were plated on day 0. **C,** Cell proliferation assay of Panc1 cells treated with vemurafenib (10 μmol/L). A total of 1×10^5 cells were plated on day 0. **D,** Cell proliferation assay of MiaPaca2 cells treated with vemurafenib (10 μmol/L). A total of 1×10^5 cells were plated on day 0. **E,** Mass spectrometry: PHGDH protein expression in pancreatic cancer cells treated with DMSO or vemurafenib (10 μmol/L; $n = 3$). **F,** Mass spectrometry: PSAT1 protein expression in pancreatic cancer cells treated with DMSO or vemurafenib (10 μmol/L; $n = 3$). (*Continued on the following page.*)

glutamine rather than glucose for proliferation. Interestingly, glutamate, catalyzed from glutamine, is a precursor of the second step of the serine biosynthesis pathway. The enzyme PSAT1 catalyzes the conversion of glutamate to α-ketoglutarate during the conversion of 3-phosphohydroxypyruvate to phosphoserine. We postulate that serine synthesis is active in SK-MEL-28VR1 cells potentially because of the described switch to oxidative metabolism during proliferation. Further studies are needed to examine the dependency of SK-MEL-28VR1 cells to glutamine.

FAM129B was identified as one of the most differentially expressed proteins between the two cell lines with respect to vemurafenib treatment. FAM129B is phosphorylated on 4 serine residues by the B-RAF/MAPKK/ERK signaling cascade (33) and is known to be dispersed throughout the cytoplasm of melanoma cells only under conditions when the MAPK pathway is active.

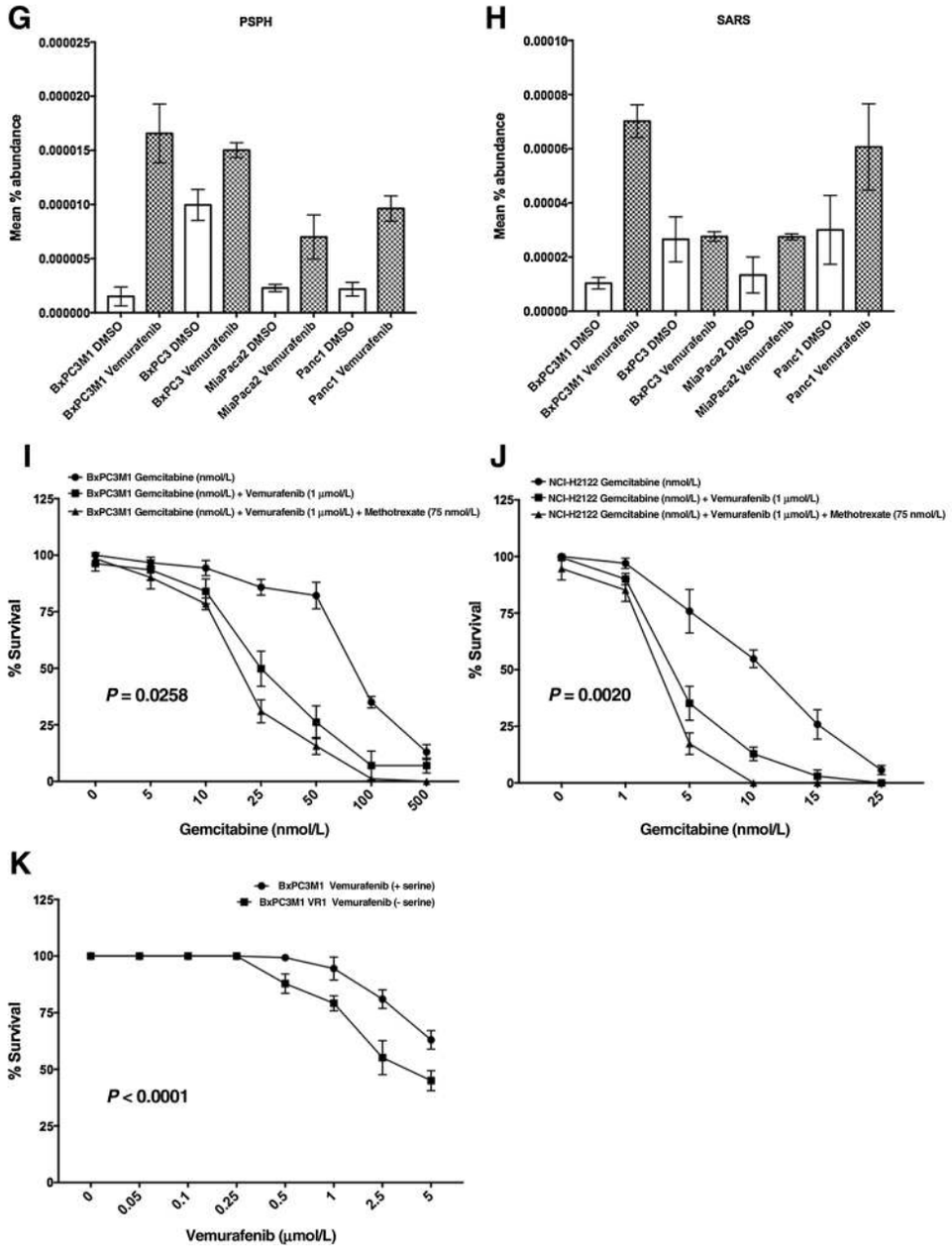

Figure 5.

(*Continued.*) **G,** Mass spectrometry: PSPH protein expression in pancreatic cancer cells treated with DMSO or vemurafenib (10 μmol/L; $n = 3$). **H,** Mass spectrometry: SARS protein expression in pancreatic cancer cells treated with DMSO or vemurafenib (10 μmol/L; $n = 3$). **I,** Colony formation assays of BxPC3M1 cells following treatments with differential doses of gemcitabine ± vemurafenib (1 μmol/L) ± methotrexate (75 nmol/L; $n = 3$; $P = 0.0258$). **J,** Colony formation assays of NCI-H2122 cells following treatments with differential doses of gemcitabine ± vemurafenib (1 μmol/L) ± methotrexate (75 nmol/L) ($n = 3$; $P = 0020$). **K,** Colony formation assays of BxPC3M1 cells following treatments with differential doses of vemurafenib ± serine ($n = 3$; $P < 0.0001$).

Smalley and colleagues showed that FAM129B overexpression increased the invasive potential of melanoma cells (34). FAM129B affects multiple signaling pathways in melanoma downstream of the MAPK cascade (18). In MS, immunoblotting, and IF assays, cytoplasmic FAM129B protein abundance increased in SK-MEL-28VR1 cells following vemurafenib treatment, but decreased in SK-MEL-28 cells. Therefore, FAM129B protein trends in our assays suggested that vemurafenib induced MAPK pathway activation in SK-MEL-28VR1 cells but not in parental cells. Furthermore, MAPK activation suggested vemurafenib may induce cell proliferation in SK-MEL-28VR1 cells supporting the observation of serine synthesis induction. We are currently investigating FAM129B as a potential biomarker for vemurafenib resistance in metastatic melanoma cells.

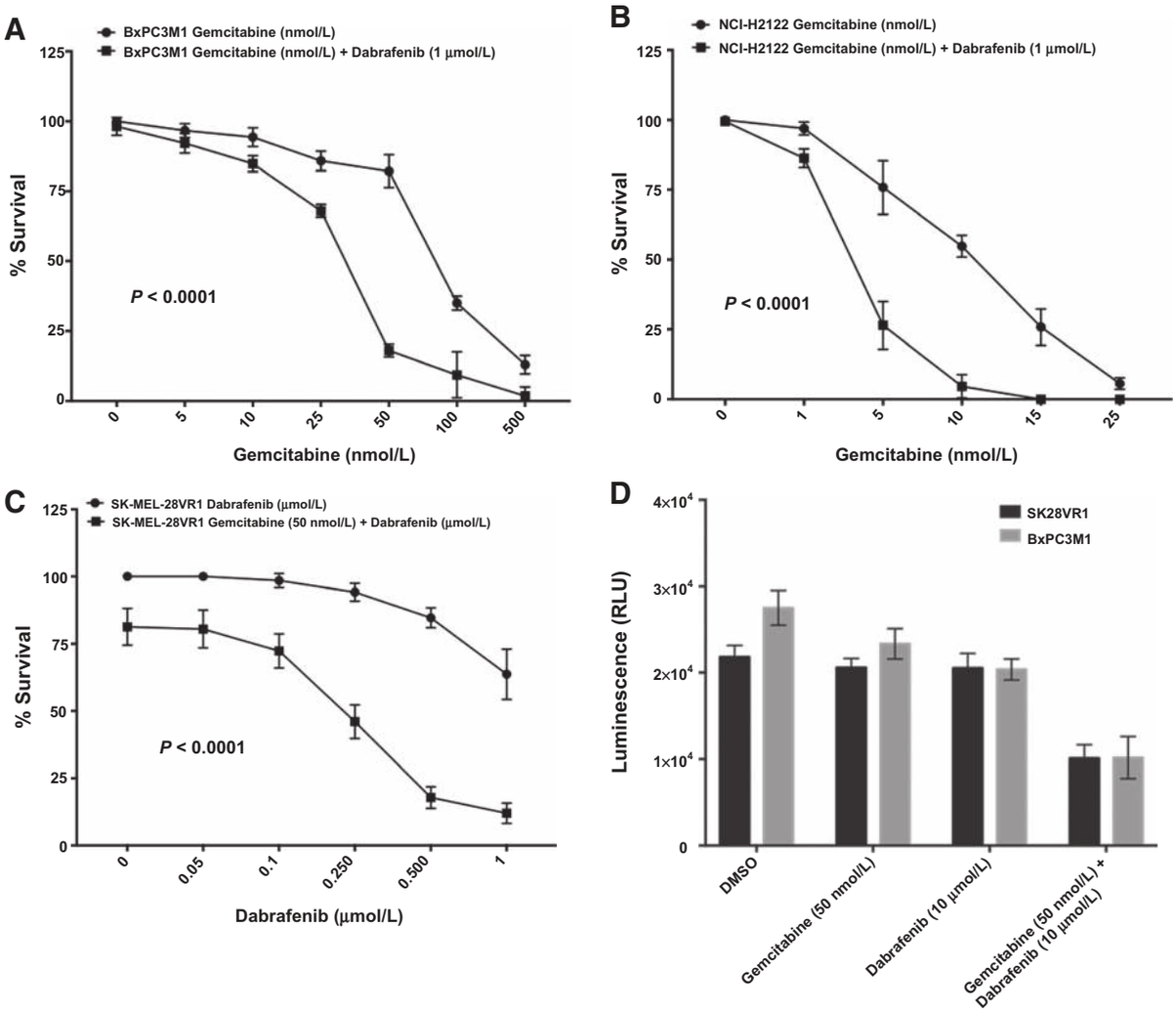

Figure 6.

Dabrafenib induced sensitization of BxPC3M1, NCI-H2122, and SK-MEL-28VR1 cells to gemcitabine. **A,** Colony formation assays of BxPC3M1 cells following treatments with differential doses of gemcitabine ± dabrafenib (1 μmol/L; $n = 3$; $P < 0.0001$). **B,** Colony formation assays of NCI-H2122 cells following treatments with differential doses of gemcitabine ± dabrafenib (1 μmol/L; $n = 3$; $P < 0.0001$). **C,** Colony formation assays of BxPC3M1 cells following treatments with differential doses of dabrafenib ± gemcitabine (50 nmol/L; $n = 3$; $P < 0.0001$). **D,** 3D spheroid assays: 5000 cells were plated on day 0. Drugs were added on day 3. On day 4, gemcitabine (50 nmol/L) was washed out and dabrafenib (10 μmol/L) was added to the combination treatment wells.

The folate cycle is known to contribute to nucleotide pool replenishment during cell proliferation, and DNA damage induces the production of nucleotides. Moreover, serine synthesis enzyme levels have been shown to increase under conditions of DNA damage and genomic instability (21). We tested several DNA-damaging agents as sensitizers of SK-MEL-28VR1 cells to vemurafenib. Gemcitabine was identified as a sensitizer when SK-MEL-28VR1 cells were pretreated with the drug before addition of vemurafenib. Combination index calculations revealed synergy between gemcitabine and vemurafenib in SK-MEL-28VR1 cells. Gemcitabine is a deoxycytidine analogue and is the primary chemotherapy against multiple tumor types including pancreatic (35, 36) and lung cancers (37, 38). Gemcitabine causes DNA double strand breaks (DSB) as a result of replication fork collapse in the S-phase of the cell cycle in p53-mutated cells or induces apoptosis through PUMA (39) and Bax (40) mediated cell death programs in G_1 in p53 WT cells. However, mutations commonly occurring in p53 and other genes of pancreatic and lung cancer tumor cells (41) drive acquired resistance to gemcitabine (42, 43) resulting in low disease-free survival (44, 45). The p53-mutated cancer cells become arrested in S-phase following treatment with gemcitabine at nmol/L doses but do not die, whereas p53 WT cells die following G_1 arrest at identical doses (46). Mutations in gatekeeper genes like p53, BRAF, and KRAS are common events in natural cancer cell progression (47); therefore, the innate ability of cancer cells to resist the DNA-damaging effects of drugs as they progress towards metastasis is especially problematic.

The order of drug addition was critical to the success of our gemcitabine + vemurafenib combination in SK-MEL-28VR1 cells.

We postulate that SK-MEL-28VR1 cells are arrested in S-phase because of gemcitabine-induced DSBs. As a result, when we treat arrested cells with vemurafenib, the MAPK cascade is activated inducing serine biosynthesis and the folate cycle. We believe that these series of events ultimately lead to cell death in SK-MEL-28VR1 cells. Further experimentation is warranted to fully characterize SK-MEL-28VR1 cell death via the gemcitabine + vemurafenib combination. We postulate that DNA damage induces cell-cycle arrest in SK-MEL28VR1 cells for DNA repair to commence, activating the folate cycle and nucleotide synthesis. While cells are arrested, *BRAF* V600E inhibitor treatment activates the MAPK pathway inducing serine synthesis and nucleotide synthesis. Ultimately, two conflicting pathways depleting the nucleotide pool of cells induce cell death.

Next, we replicated our vemurafenib studies in BRAF WT cancer cell lines that are naturally nonresponsive to the drug. as vemurafenib is known to increase proliferation of cells with BRAF WT backgrounds, we postulate that serine biosynthesis might be critical for cell survival and proliferation under vemurafenib treatment conditions. We examined multiple cancer cell lines that are BRAF WT and are intrinsically resistant to vemurafenib. We tested pancreatic, NSCL, breast, and colon cancer cells. Indeed, MS studies identified the serine biosynthesis pathway as greatly induced in BRAF WT pancreatic cancer cells in response to vemurafenib treatments. BxPC3M1 cells had the highest increase in serine synthesis enzymes of the pancreatic cancer cell lines with drug treatment. Then, we tested gemcitabine at variable doses and kept the vemurafenib dose constant. One pancreatic cancer

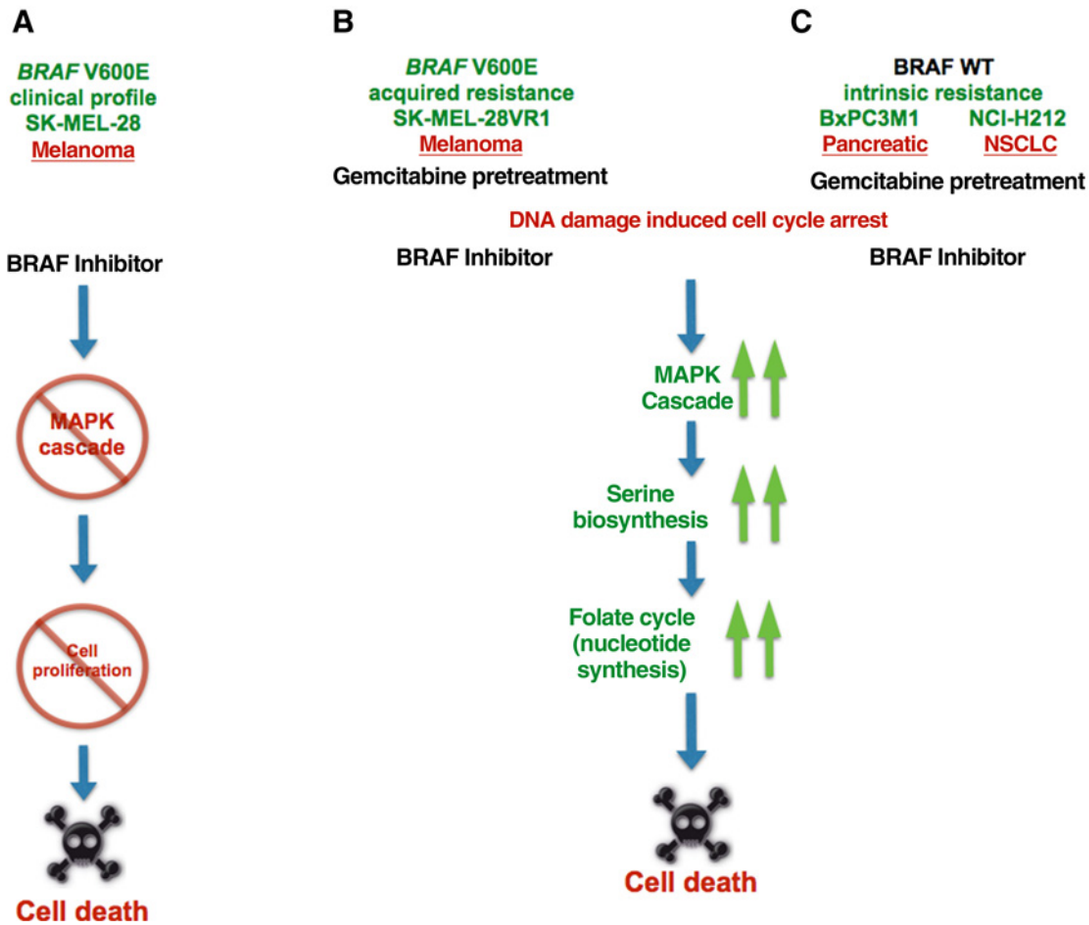

Figure 7.

Schematic of cancer cell sensitization via sequential combination treatment with gemcitabine and a *BRAF* V600E inhibitor. Cascade A represents SK-MEL-28 cellular response to *BRAF* V600E inhibitors (BRAFi) within the *BRAF* V600E mutation. Cascade B represents acquired BRAFi-resistant SK-MEL-28VR1 cellular response to BRAFi within the mutation profile. Acquired resistance causes a paradoxical induction of the MAPK cascade without gemcitabine pretreatment. Gemcitabine pretreatment followed by BRAFi leads to induction of the MAPK cascade and induction of serine synthesis while cells are arrested. Induction of serine synthesis leads to an induction of the folate cycle for nucleotide synthesis. These series of events lead to cell death due to conflicting activation of cellular signaling pathway causing cell-cycle arrest signal from gemcitabine-induced DNA damage and activation of MAPK signaling pathway by BRAF inhibitors. Cascade C shows sensitization of BRAF WT pancreatic cancer BxPC3M1 and NSCLC NCI-H2122 cells to BRAF inhibitors by gemcitabine pretreatment. In these BRAF WT cell lines, gemcitabine induces cell-cycle arrest. Addition of BRAF inhibitors to the arrested cells induces the MAPK cascade, leading to increased serine synthesis and folate synthesis. These series of events lead to cell death due to conflicting activation of cellular signaling pathway causing cell-cycle arrest from gemcitabine-induced DNA damage and activation of MAPK signaling pathway by BRAF inhibitors. The actual mechanism of cell death is as yet unknown.

(BxPC3M1) and 1 NSCLC (NCI-H2122) cell line were sensitized to the combination treatments. As seen in SK-MEL-28VR1 cells, the order of drug addition was critical for sensitization. Gemcitabine pretreatment was necessary for successful sensitization. These data showed that 5,000 nmol/L dose of gemcitabine alone caused cell death and adding in 1 μmol/L vemurafenib reduces gemcitabine toxicity. However, lower gemcitabine doses (25 nmol/L–1,000 nmol/L) synergized with vemurafenib. At the lowest doses of gemcitabine (5 nmol/L and 10 nmol/L), the two drugs have a competitive relationship. These doses of gemcitabine appear too low to have any effect on our CI plots. We believe that cell-cycle arrest is necessary for vemurafenib-induced cell death in BxPC3M1 cells. In addition, BxPC3M1 cell proliferation was induced by vemurafenib treatment. Serine depletion experiments demonstrated the need for baseline levels of extracellular serine for BxPC3M1 vemurafenib resistance. Importantly, gemcitabine sensitized SK-MEL-28VR1, BxPC3M1, and NCI-H2122 cells to another *BRAF*V600E inhibitor dabrafenib. Collectively, our data showed that acquired resistance of SK-MEL-28VR1 cells and intrinsic resistance of BxPC3M1 and NCI-H2122 cells to BRAFis can be reversed via gemcitabine addition. Gemcitabine and vemurafenib showed synergy in SK-MEL-28VR1 and BxPC3M1 cells.

As we did not observe sensitization with gemcitabine + vemurafenib combinations across all pancreatic cancer and NSCLC cell lines tested, we started to examine the unifying characteristics among responders, SK-MEL28VR1, BxPC3M1, and NCI-H2122 cells. However, an interesting observation we are exploring is a qualitative feature common to SK-MEL-28VR1, BxPC3M1, and NCI-H2122 cells. The cell lines have detached phenotypes. This phenotype is consistent with the detached phenotype of mesenchymal cancer cells. There is precedence for epithelial-to-mesenchymal transition (EMT) being a path to vemurafenib resistance (48, 49). We postulate that metastatic potential as well as mutational profile could be critical determinants of cell sensitivity to the gemcitabine + vemurafenib combination illuminating the potential for personalized therapies.

This study has identified serine biosynthesis as a critical determinant of BRAF inhibitor resistance in cancer cells. In addition, we have demonstrated methotrexate as a sensitizer of melanoma cells to *BRAF* V600E inhibitors. We have demonstrated gemcitabine pretreatment as a sensitizer of cancer cells to vemurafenib or dabrafenib. The relationships between gemcitabine and vemurafenib, or gemcitabine and dabrafenib are currently being explored to further enhance cell sensitivity. Ultimately, our studies demonstrate the successful use of quantitative proteomic profiling to identify novel protein and pathway targets that can be disrupted to reverse resistance of *BRAF* V600E and BRAF WT cancer cells to BRAF inhibitors, vemurafenib or dabrafenib. Figure 7 summarizes the totality of our discovery.

Disclosure of Potential Conflicts of Interest

A.J. Andrews has ownership interest (including patents) in Evol Science. T.J. Yen is a consultant/advisory board member for Evol Science. No potential conflicts of interest were disclosed by the other authors.

Authors' Contributions

Conception and design: K.C. Ross, V. Bhattacharjee
Development of methodology: A.J. Andrews, V. Bhattacharjee
Acquisition of data (provided animals, acquired and managed patients, provided facilities, etc.): K.C. Ross, T.J. Yen, V. Bhattacharjee
Analysis and interpretation of data (e.g., statistical analysis, biostatistics, computational analysis): K.C. Ross, C.D. Marion, T.J. Yen, V. Bhattacharjee
Writing, review, and/or revision of the manuscript: T.J. Yen, V. Bhattacharjee
Administrative, technical, or material support (i.e., reporting or organizing data, constructing databases): K.C. Ross, V. Bhattacharjee
Study supervision: T.J. Yen, V. Bhattacharjee

Acknowledgments

We thank J. Hittle, A. Bellacosa, R. Tricarico, S. Alvarez, P. Donahoe, T. Hall, D. Pepin, and J. Driscoll.

Grant Support

K.C. Ross, C.D. Marion, A.J. Andrews, and V. Bhattacharjee were supported by private funding provided by Evol Science, LLC. T.J. Yen was partly supported by NIHCA191956, core grant CA06927, PA Cure, and a generous gift by Mrs. C. Greenberg.

The costs of publication of this article were defrayed in part by the payment of page charges. This article must therefore be hereby marked *advertisement* in accordance with 18 U.S.C. Section 1734 solely to indicate this fact.

Received November 23, 2016; revised April 4, 2017; accepted April 24, 2017; published OnlineFirst May 12, 2017.

References

1. Sala E, Mologni L, Truffa S, Gaetano C, Bollag GE, Gambacorti-Passerini C. BRAF silencing by short hairpin RNA or chemical blockade by PLX4032 leads to different responses in melanoma and thyroid carcinoma cells. Mol Cancer Res 2008;6:751–9.
2. Halaban R, Zhang W, Bacchiocchi A, Cheng E, Parisi F, Ariyan S, et al. PLX4032, a selective BRAF(V600E) kinase inhibitor, activates the ERK pathway and enhances cell migration and proliferation of BRAF melanoma cells. Pigment Cell Melanoma Res 2010;23:190–200.
3. Hatzivassiliou G, Song K, Yen I, Brandhuber BJ, Anderson DJ, Alvarado R, et al. RAF inhibitors prime wild-type RAF to activate the MAPK pathway and enhance growth. Nature 2010;464:431–5.
4. Poulikakos PI, Zhang C, Bollag G, Shokat KM, Rosen N. RAF inhibitors transactivate RAF dimers and ERK signalling in cells with wild-type BRAF. Nature 2010;464:427–30.
5. Moriceau G, Hugo W, Hong A, Shi H, Kong X, Yu CC, et al. Tunable-combinatorial mechanisms of acquired resistance limit the efficacy of BRAF/MEK cotargeting but result in melanoma drug addiction. Cancer Cell 2015;27:240–56.
6. Sullivan RJ, Flaherty KT. BRAF in melanoma: pathogenesis, diagnosis, inhibition, and resistance. J Skin Cancer 2011;2011:423239.
7. Girotti MR, Pedersen M, Sanchez-Laorden B, Viros A, Turajlic S, Niculescu-Duvaz D, et al. Inhibiting EGF receptor or SRC family kinase signaling overcomes BRAF inhibitor resistance in melanoma. Cancer Discov 2013;3:158–67.
8. Corcoran RB, Dias-Santagata D, Bergethon K, Iafrate AJ, Settleman J, Engelman JA. BRAF gene amplification can promote acquired resistance to MEK inhibitors in cancer cells harboring the BRAF V600E mutation. Sci Signal 2010;3:ra84.
9. Flaherty KT, Infante JR, Daud A, Gonzalez R, Kefford RF, Sosman J, et al. Combined BRAF and MEK inhibition in melanoma with BRAF V600 mutations. N Engl J Med 2012;367:1694–703.
10. Abdel-Wahab O, Klimek VM, Gaskell AA, Viale A, Cheng D, Kim E, et al. Efficacy of intermittent combined RAF and MEK inhibition in a patient with concurrent BRAF- and NRAS-mutant malignancies. Cancer Discov 2014;4:538–45.
11. Atefi M, von Euw E, Attar N, Ng C, Chu C, Guo D, et al. Reversing melanoma cross-resistance to BRAF and MEK inhibitors by co-targeting the AKT/mTOR pathway. PLoS One 2011;6:e28973.
12. Greger JG, Eastman SD, Zhang V, Bleam MR, Hughes AM, Smitheman KN, et al. Combinations of BRAF, MEK, and PI3K/mTOR inhibitors overcome

acquired resistance to the BRAF inhibitor GSK2118436 dabrafenib, mediated by NRAS or MEK mutations. Mol Cancer Ther 2012;11:909–20.
13. Long GV, Stroyakovskiy D, Gogas H, Levchenko E, De Braud F, Larkin J, et al. Dabrafenib and trametinib versus dabrafenib and placebo for Val600 BRAF-mutant melanoma: a multicentre, double-blind, phase 3 randomised controlled trial. Lancet 2015;386:444–51.
14. Gowrishankar K, Snoyman S, Pupo GM, Becker TM, Kefford RF, Rizos H. Acquired resistance to BRAF inhibition can confer cross-resistance to combined BRAF/MEK inhibition. J Invest Dermatol 2012;132:1850–9.
15. Villanueva J, Infante JR, Krepler C, Reyes-Uribe P, Samanta M, Chen HY, et al. Concurrent MEK2 mutation and BRAF amplification confer resistance to BRAF and MEK inhibitors in melanoma. Cell Rep 2013;4:1090–9.
16. Snell K, Natsumeda Y, Eble JN, Glover JL, Weber G. Enzymic imbalance in serine metabolism in human colon carcinoma and rat sarcoma. Br J Cancer 1988;57:87–90.
17. Chou TC, Martin N. CompuSyn software for drug combinations and for general dose effect analysis, and user's guide. Paramus, NJ: ComboSyn, Inc.; 2007.
18. Conrad W, Major MB, Cleary MA, Ferrer M, Roberts B, Marine S, et al. FAM129B is a novel regulator of Wnt/β-catenin signal transduction in melanoma cells. F1000Research 2013;2:134.
19. Tedeschi PM, Markert EK, Gounder M, Lin H, Dvorzhinski D, Dolfi SC, et al. Contribution of serine, folate and glycine metabolism to the ATP, NADPH and purine requirements of cancer cells. Cell Death Dis 2013; 4:e877.
20. Sneader W. Drug discovery: a history. West Sussex, England: John Wiley & Sons; 2006.
21. Markkanen E, Fischer R, Ledentcova M, Kessler BM, Dianov GL. Cells deficient in base-excision repair reveal cancer hallmarks originating from adjustments to genetic instability. Nucleic Acids Res 2015;43:3667–79.
22. Hayashi H, Kurata T, Nakagawa K. Gemcitabine: efficacy in the treatment of advanced stage nonsquamous non-small cell lung cancer. Clin Med Insights Oncol 2011;5:177–84.
23. Menzies AM, Long GV, Murali R. Dabrafenib and its potential for the treatment of metastatic melanoma. Drug Des Devel Ther 2012;6:391–405.
24. Spagnolo F, Ghiorzo P, Orgiano L, Pastorino L, Picasso V, Tornari E, et al. BRAF-mutant melanoma: treatment approaches, resistance mechanisms, and diagnostic strategies. Onco Targets Ther 2015;8:157–68.
25. Labuschagne CF, van den Broek NJF, Mackay GM, Vousden KH, Maddocks ODK. Serine, but not glycine, supports one-carbon metabolism and proliferation of cancer cells. Cell Rep 2014;7:1248–58.
26. Mattaini KR, Sullivan MR, Vander Heiden MG. The importance of serine metabolism in cancer. J Cell Biol 2016;214:249–57.
27. Possemato R, Marks KM, Shaul YD, Pacold ME, Kim D, Birsoy K, et al. Functional genomics reveal that the serine synthesis pathway is essential in breast cancer. Nature 2011;476:346–50.
28. Beroukhim R, Mermel CH, Porter D, Wei G, Raychaudhuri S, Donovan J, et al. The landscape of somatic copy-number alteration across human cancers. Nature 2010;463:899–905.
29. Locasale JW, Grassian AR, Melman T, Lyssiotis CA, Mattaini KR, Bass AJ, et al. Phosphoglycerate dehydrogenase diverts glycolytic flux and contributes to oncogenesis. Nat Genet 2011;43:869–74.
30. DeNicola GM, Chen PH, Mullarky E, Sudderth JA, Hu Z, Wu D, et al. NRF2 regulates serine biosynthesis in non–small cell lung cancer. Nat Genet 2015;47:1475–81.
31. Mullarky E, Mattaini KR, Vander Heiden MG, Cantley LC, Locasale JW. PHGDH amplification and altered glucose metabolism in human melanoma. Pigment Cell Melanoma Res 2011;24:1112–5.
32. Baenke F, Chaneton B, Smith M, Van Den Broek N, Hogan K, Tang H, et al. Resistance to BRAF inhibitors induces glutamine dependency in melanoma cells. Mol Oncol 2016;10:73–84.
33. Old WM, Shabb JB, Houel S, Wang H, Couts KL, Yen C, et al. Functional proteomics identifies targets of phosphorylation by B-Raf signaling in melanoma. Mol Cell 2009;34:115.
34. Smalley KS, Haass NK, Brafford PA, Lioni M, Flaherty KT, Herlyn M. Multiple signaling pathways must be targeted to overcome drug resistance in cell lines derived from melanoma metastases. Mol Cancer Ther 2006;5:1136–44.
35. Feldmann G, Rauenzahn S, Maitra A. In vitro models of pancreatic cancer for translational oncology research. Expert Opin Drug Discov 2009;4: 429–43.
36. Morgan M, El Shaikh MA, Abu-Isa E, Davis MA, Lawrence TS. Radiosensitization by gemcitabine fixed-dose-rate infusion versus bolus injection in a pancreatic cancer model. Transl Oncol 2008;1:44–9.
37. Brodowicz T, Krzakowski M, Zwitter M, Tzekova V, Ramlau R, Ghilezan N, et al. Cisplatin and gemcitabine first-line chemotherapy followed by maintenance gemcitabine or best supportive care in advanced non-small cell lung cancer: a phase III trial. Lung Cancer 2006;52:155–63.
38. Tham LS, Wang L, Soo RA, Lee SC, Lee HS, Yong WP, et al. A pharmacodynamic model for the time course of tumor shrinkage by gemcitabine + carboplatin in non-small cell lung cancer patients. Clin Cancer Res 2008;14:4213–8.
39. Qian H, Wang T, Naumovski L, Lopez CD, Brachmann RK. Groups of p53 target genes involved in specific p53 downstream effects cluster into different classes of DNA binding sites. Oncogene 2002;21:7901–11.
40. Chipuk JE, Kuwana T, Bouchier-Hayes L, Droin NM, Newmeyer DD, Schuler M, et al. Direct activation of Bax by p53 mediates mitochondrial membrane permeabilization and apoptosis. Science 2004;303:1010–4.
41. Muller PA, Vousden KH. Mutant p53 in cancer: new functions and therapeutic opportunities. Cancer Cell 2014;25:304–17.
42. Bergman AM, Pinedo HM, Peters GJ. Determinants of resistance to 2′,2′-difluorodeoxycytidine (gemcitabine). Drug Resist Updat 2002;5:19–33.
43. Ohhashi S, Ohuchida K, Mizumoto K, Fujita H, Egami T, Yu J, et al. Down-regulation of deoxycytidine kinase enhances acquired resistance to gemcitabine in pancreatic cancer. Anticancer Res 2008;28:2205–12.
44. Paulson AS, Tran Cao HS, Tempero MA, Lowy AM. Therapeutic advances in pancreatic cancer. Gastroenterology 2013;144:1316–26.
45. Wolfgang CL, Herman JM, Laheru DA, Klein AP, Erdek MA, Fishman EK, et al. Recent progress in pancreatic cancer. CA Cancer J Clin 2013;63: 318–48.
46. Senturk E, Manfredi JJ. p53 and cell cycle effects after DNA damage. Methods Mol Biol 2013;962:49–61.
47. Meacham CE, Morrison SJ. Tumour heterogeneity and cancer cell plasticity. Nature 2013;501:328–37.
48. Fedorenko IV, Abel EV, Koomen JM, Fang B, Wood ER, Chen YA, et al. Fibronectin induction abrogates the BRAF inhibitor response of BRAF V600E/PTEN-null melanoma cells. Oncogene 2016;35:1225–35.
49. Li FZ, Dhillon AS, Anderson RL, McArthur G, Ferrao PT. Phenotype switching in melanoma: implications for progression and therapy. Front Oncol 2015;5:31.